

Safety of Intra-Arterial Injection With Tumor-Activated T Cells to the Rabbit Brain Evaluated by MRI and SPECT/CT

Johan Lundberg,*† Emma Jussing,*† Zhenjiang Liu,‡ Qingda Meng,‡ Martin Rao,‡ Erik Samén,*† Rikard Grankvist,*† Peter Damberg,*§ Ernest Doodoo,‡ Markus Maeurer,‡¶ and Staffan Holmin*†

*Department of Clinical Neuroscience, Karolinska Institutet, Stockholm, Sweden

†Department of Neuroradiology, Karolinska University Hospital, Stockholm, Sweden

‡Therapeutic Immunology Unit, Department of Laboratory Medicine, Karolinska Institutet, Stockholm, Sweden

§Karolinska Experimental Research and Imaging Center, Karolinska University Hospital, Stockholm, Sweden

¶Centre for Allogeneic Stem Cell Transplantation (CAST), Karolinska University Hospital Huddinge, Stockholm, Sweden

Glioblastoma multiforme (GBM) is the most common and most severe form of malignant gliomas. The prognosis is poor with current combinations of pharmaceutical, radiotherapy, and surgical therapy. A continuous search for new treatments has therefore been ongoing for many years. Therapy with tumor-infiltrating lymphocytes (TILs) is a clinically promising strategy to treat various cancers, including GBM. An endovascular intra-arterial injection of TILs as a method of delivery may, instead of intravenous infusion, result in better retention of effector cells within the tumor. Prior to clinical trials of intra-arterial injections with any cells, preclinical safety data with special emphasis on embolic–ischemic events are necessary to obtain. We used native rabbits as a model for intra-arterial injections with routine clinical catheter material and a clinical angiography suite. We selectively infused a total dose of 20 million activated T cells at a cell concentration of 4,000 cells/ μ l over 8 min of injection time. The rabbits were evaluated for ischemic lesions by 9.4 T magnetic resonance imaging (MRI) ($n=6$), and for tracking of injected cells, single-photon emission computed tomography/computed tomography (SPECT/CT) was used ($n=2$). In this study, we show that we can selectively infuse activated T cells to a CNS volume of 3.5 cm³ (estimated from the volumetric MRI) without catastrophic embolic–ischemic adverse events. We had one adverse event with a limited basal ganglia infarction, probably due to catheter-induced mechanical occlusion of one of the lateral lenticulostriatal arteries. The cells pass through the native brain without leaving SPECT signals. The cells then, over the first hours, end up in the liver to a large extent and to a lesser degree by the spleen, pancreas, and kidneys. Virtually no uptake could be detected in the lungs. This indicates a difference in biodistribution as opposed to other cell types when infused intravenously.

Key words: Endovascular; Intra-arterial (IA); Tumor-infiltrating lymphocytes (TILs); Magnetic resonance imaging (MRI); Single-photon emission computed tomography/computed tomography (SPECT/CT); Rabbit

INTRODUCTION

Glioblastoma multiforme (GBM) is the most severe and most common form of malignant glioma. The prognosis is poor with a 27.2% survival rate at 2 years and a 9.8% survival rate at 5 years for patients treated with radiotherapy with concomitant temozolomide¹. Further treatment options are thus warranted. One of the promising treatment options that are now emerging in clinical trials is the use of cellular therapy targeting cancer-associated mutations, for example, the splice variant of epidermal growth factor receptor variant III (EGFRvIII) in GBM². Previous trials in patients with GBM with cytokine-activated T cells or tumor-infiltrating lymphocytes (TILs) showed safety

and suggested clinical efficacy^{3–7}. More recent data, using TILs from patients with solid tumors, show that clinically relevant antitumor immune responses target “private” mutations from the patient’s tumor^{8,9}. We have previously reported that TILs can be successfully expanded in vitro up to 10¹⁰ cells using a cocktail of interleukin-2 (IL-2), IL-15, and IL-21¹⁰. Th1 cells are also expanded, along with increased expression of C-X-C chemokine receptor type 3 (CXCR3) among CD8⁺ and CD4⁺ T cells that enables increased access to tumor tissue. Thus, the passive transfer of TILs from patients with GBM may therefore represent a viable clinical treatment option and further achieve biologically meaningful antitumor effects.

Received July 4, 2016; final acceptance November 2, 2016. Online prepub date: October 7, 2016.

Address correspondence to Johan Lundberg, M.D., Ph.D., Department of Neuroradiology, Karolinska University Hospital, Solna, 171 76 Stockholm, Sweden. Tel: +46-73-6258594; E-mail: j.lundberg@ki.se

For cell-based treatment approaches, the mechanism of delivery is of greater significance compared to pharmacological approaches¹¹. Local delivery of cells could have a potentially higher therapeutic effect as opposed to systemic delivery by the intravenous (IV) route. With modern imaging techniques, the arteries and veins of the body can be considered “internal routes” that are easily and routinely navigated by endovascular catheters to the central nervous system (CNS) for both diagnostic and therapeutic reasons. With a modern microcatheter, it is possible to perform selective injections of pharmacological substances, viral vectors, and cell preparations.

The principal routes for cell administration are intraparenchymal, IV, and intra-arterial (IA) injections. There are also mostly preclinical reports concerning intracerebroventricular injections; however, there is a debate concerning feasibility and safety. A significant concern is that injected cells could adhere to the ventricular wall and cause obstructive hydrocephalus¹². The least invasive method is the IV infusion used in clinical practice for bone marrow transplantations for many years^{13–15}. A significant concern is that in some cell types, a large fraction of the infused cells gets trapped in the pulmonary circulation, and only a small fraction of the cells actually enter the target organ^{16,17}. One older study using genetically marked cells showed that most T cells after the first lung passage stay for approximately 3 days in the lung tissue¹⁸ and will then ultimately home to the target tissue. Only a fraction of TILs may be directed against clinically relevant targets⁸; therefore, the delivery of tumor-associated antigen (TAA)¹-reactive T cells into the tumor may be of clinical relevance, avoiding pulmonary passage and potential dilution of antitumor-directed frequencies. Further complicating IV infusions of TILs is the common complication of thrombotic microangiopathy among patients undergoing whole-body irradiation and stem cell transplantation. Thrombotic microangiopathy has been reported in approximately 30% of patients with metastatic melanoma receiving IV TIL infusion¹⁹. In addition, patients with resectable GBM appear to have a high propensity to develop venous thrombosis²⁰, thus raising concerns for IV infusions of TILs. On the opposite side of the invasiveness spectra is the direct parenchymal injection through stereotaxic means to the CNS. However, there are significant risks connected with the stereotaxic puncture of the CNS²¹, and on the anecdotal level of evidence, patients do not prefer the direct puncture as opposed to a minimally invasive approach.

An IA approach gives a high-concentration first-passage effect. Further, the entire injected cell volume will have the possibility to interact with the postcapillary endothelia of the intended treatment target. The primary benefit of the IA route is that more cells reach the desired target compared to IV infusions as has been

shown in different pathological conditions^{22,23}. The cost of IA injections is a minor increase of risk for ischemic adverse events. As a comparison, the risk of diagnostic angiography for permanent neurologic complication is reported at maximally 0.5%, with the highest risk in older patients with vascular disease²⁴. Furthermore, if large amounts of contrast agent is injected, a transient opening of the blood–brain barrier (BBB) can occur²⁵. Based on previous clinical experience with patients with metastatic cancer, local delivery of TILs into the tumor generally appears to be more efficacious than systemic delivery via the IV route²⁵. The targeted delivery via endovascular IA injection may therefore be of noteworthy biological and clinical relevance.

Prior to launching clinical trials of IA cell injections, several key issues need to be investigated in the preclinical setting. Several technical aspects such as cell volume, cell concentration, and compatibility with the intended catheter system should be evaluated¹². One risk factor is shear stress that the catheter walls create on the cell suspension¹². Further, especially for IA injections, the safety of the procedure should be tested with special emphasis on the risk for cell aggregation and/or embolization and the subsequent risk for ischemic stroke²⁷. Since cell suspensions differ substantially, this must be performed on a well-characterized cell population that is the same as the intended cells to be used in clinical trials and subsequent clinical practice.

The purpose of this study was to evaluate the safety of IA injection of activated T cells to a native rabbit brain using the intended setup of clinical microcatheters and angiography suite. The animals were evaluated with 9.4 T magnetic resonance imaging (MRI), and cells were tracked with single-photon emission computed tomography/computed tomography (SPECT/CT) fusion imaging.

MATERIALS AND METHODS

Ethics Statement

All animal studies were conducted according to the Karolinska Institutet guidelines of animal experiments on small rodents and rabbits. The studies were approved by the regional ethics committee for animal research at the Karolinska University Hospital (Stockholm, Sweden). Expansion of human TILs was approved by the regional ethical review board at Karolinska Institutet, Stockholm, Sweden (Diary No. 2013/576-31).

TIL Expansion

Glioma tumor tissue was harvested in the course of tumor surgery at the Department of Neuro-Oncology at Karolinska Hospital. Tumor tissue was immediately transferred to CellGro (CellGenix, Freiburg, Germany) medium supplemented with 5% pooled human AB serum

(Innovative Research, Novi, MI, USA). According to the manufacturer, this medium can be used for dendritic cell as well as T-cell expansion protocols. Tumor tissue was dissected into fragments (approximately 1–2 mm³) using a sterile scalpel or processed into a tissue homogenate using a Medimachine (BD Biosciences, San Jose, CA, USA). Tissue fragments of the cell suspension were washed two times with phosphate-buffered saline (PBS) and cultured in 24-well plates in good manufacturing practice (GMP) serum-free DC medium (CellGenix) plus 5% pooled human AB serum (Innovative Research) supplemented with recombinant IL-2 (1,000 IU/ml), IL-15 (10 ng/ml), and IL-21 (10 ng/ml) (ProSpec, Ness-Ziona, Israel). The medium was changed when necessary. Irradiated (55 Gy) feeder cells [allogeneic peripheral blood mononuclear cells (PBMCs)] at the ratio of 1:10 (feeder cells/TILs) were added on day 7. OKT3 (anti-CD3 monoAb; BioLegend, San Diego, CA, USA) was used at 10 ng/ml as TILs were visible. TILs were transferred into six-well plates; as they covered >70% of the 24-well surface, they could be further expanded in G-Rex flasks (Wilson Wolf, New Brighton, MN, USA) using 30 ng of OKT3/ml and irradiated (55 Gy) allogeneic feeder cells at the ratio of 1:10 (feeder cells/TILs). Twenty million cells were suspended at a concentration of 4,000 cells/ μ l in vehicle of 5% human AB serum in 0.9% NaCl solution, while the infusion was performed at room temperature.

Immunophenotyping of TILs

TILs were stained with the following Ab cocktail: anti-CD3 Brilliant Violet 570 (BioLegend), anti-CD4 Brilliant Violet 510 (BioLegend), anti-CD8a APC-Cy7 (BD Biosciences), anti-CD45RA Percp Cy5.5 (BioLegend), anti-CCR7 Brilliant Violet 421 (BioLegend), anti-CXCR3 FITC (BioLegend), anti-CCR4 AF647 (BD Biosciences), and CCR6 PE CF594 (BD Biosciences). After 15 min, T cells were washed in PBS with 1% fetal bovine serum (FBS) (Life Technologies, Carlsbad, CA, USA) and analyzed using a FACSAria flow cytometer (BD Biosciences, Stockholm, Sweden); data analysis was performed by FlowJo software, and the immunophenotype panel was analyzed according to the gating strategy from the study of Becattini et al.²⁸.

Animal Model

Nine female New Zealand White rabbits weighing 3.5 \pm 0.3 kg were used in the study. Procedures were performed under general anesthesia and with sterile conditions on intubated rabbits connected to a servo ventilator. Anesthesia was induced by subcutaneous injection of 0.5 ml/kg Hypnorm (fentanyl citrate, 0.315 mg/ml; fluanisone, 10 mg/ml; Janssen Pharmaceuticals, Antwerpen, Belgium) combined with 5 mg of diazepam (Actavis Group PTC, Hafnarfjordi, Iceland). Maintenance of

anesthesia was achieved by continuous IV infusion of Propofol-Lipuro (Braun Medical AB, Danderyd, Sweden) at a rate of 20 ml/h and IV injection of 0.1 ml of Hypnorm every 30 min.

All large animal angiography and endovascular intervention were performed with a Philips XD20 angiographical equipment (Philips Medical Systems, Best, The Netherlands). Visipaque 270 contrast agent (GE Healthcare, Danderyd, Sweden) was used in all angiography applications.

A 4F pediatric introducer (Terumo Medical Corporation, Tokyo, Japan) was inserted into the femoral artery through a surgical incision, and a 4F catheter (Vertebral; Cook, Bloomington, IN, USA) was navigated to the common carotid artery. A 1.2F microcatheter (Magic; Balt Extrusion, Montmorency, France) was then navigated to the internal carotid artery (ICA), and in that position 20 million cells were infused at a concentration of 4,000 cells/ μ l with a total injection time of 8 min. Angiography was performed following injection. For the positive control of infarction, a total volume of 1,000 μ l of 50:50 mixture of 40 μ m of embozene beads (Boston Scientific AB, Helsingborg, Sweden) and contrast agent (Visipaque 270; GE Healthcare) was injected in the M1 segment.

MRI

The MRI was conducted at 9.4 T in a horizontal magnet with a 30-cm-wide opening (Agilent Technologies, Yarnton, UK). A 20-cm gradient insert, capable of generating 30 G/cm gradient fields, was used together with a birdcage coil of 150-mm inner diameter for transmission (Rapid Biomedical, Rimpfing, Germany).

The rabbits were placed in the MRI-compatible bed designed for obese rats (Rapid Biomedical) in supine position. The head was secured in a semicircular surface coil designed for rat heart imaging (Rapid Biomedical), which was used for signal reception.

Diffusion-weighted imaging (DWI) was accomplished through a fat-suppressed spin echo sequence [repetition time (TR) 2.9 s, echo time (TE) 22.96 ms, number of excitations 1, matrix size 128 \times 96, field of view (FOV) 60 \times 60 mm², 27 contiguous slices of 1-mm thickness] with diffusion-weighting gradients (18.64 G/cm, 23.8 ms, gradient separation 12.9 ms, *b* value 951.8 s/mm²) applied along 12 directions and two reference images, where the diffusion-weighting gradient intensities were set to zero.

T1-weighted images were obtained using a fat-suppressed spin echo sequence (TR 700 ms, TE 15.12 ms, FOV 60 \times 60 mm², matrix size 192 \times 192, 14 slices 1 mm with 1-mm gap, repeated in 2 min 17 s, repeated with the slice package translated 1 mm in the slice select direction to keep the TR short to have T1 weighting and have complete coverage).

Images with higher spatial resolution were acquired using a fast spin echo 3D sequence (TR 800 ms, echo train length 8, kz zero 4, effective TE 31.18 ms, FOV $51.2 \times 51.2 \times 51.2$ mm³, matrix $256 \times 192 \times 192$).

The permeability of the BBB was investigated using alterations in T1-weighted images following a bolus dose of Magnevist (Bayer Pharma AG, Berlin, Germany).

Labeling Cells With Indium-111

Labeling was performed essentially according to the instructions for cell labeling provided by the indium oxinate supplier (Mallinckrodt Medical, Petten, Holland). TIL cells, 20×10^6 in buffer, 90% viable according to the trypan blue exclusion test, were centrifuged and resuspended in 2 ml of PBS. ¹¹¹In-oxinate (Mallinckrodt Medical) (20 MBq) in Tris buffer (1.4 ml) was added and allowed to react for 21 min at 36°C with occasional swirling to maintain suspension. The tubes were centrifuged, the unreacted radioactivity in the supernatant was removed, 5 ml of wash solution [10% FBS in Roswell Park Memorial Institute (RPMI) medium] was added, and the cells were resuspended with swirling. The centrifugation was repeated two more times, and the radioactivity in the cells and supernatants was measured. Labeling efficiency was ~70%. The labeled cells were resuspended in 5 ml of 5% albumin (Life Technologies) in physiological saline (9 mg/ml), thus with a concentration of 4,000 cells/ μ l for the transplantation procedure and tested for a >0.90 viability ratio with trypan blue (Thermo Fisher Scientific, Stockholm, Sweden).

SPECT/CT

The SPECT/CT system (Symbia T; Siemens GmbH, Berlin, Germany) consisted of a dual-head variable-angle γ camera equipped with low-energy high-resolution collimators and a multislice spiral CT component optimized for rapid rotation. The SPECT acquisition (128 \times 128 matrix, 81 frames, 45 s/frame) was performed using 4.5° angular steps in a 50-s time frame. For CT (158 kV, 210 mAs, B50s kernel, 512 \times 512 matrix), 0.75-mm slices were obtained. After reconstruction, SPECT images were corrected for attenuation and scatter. Both SPECT and CT axial 5-mm slices were generated using Hermes Gold 450 (Hermes Medical Solution, Stockholm, Sweden). Images were then analyzed with the OsiriX imaging software (OsiriX Foundation, Geneva, Switzerland).

RESULTS

We successfully expanded TILs from six patients with GBM in medium containing a cocktail of IL-2, IL-15, and IL-21. The TILs exhibited a median frequency of 88.4% among CD3⁺ T cells, while the median frequencies of CD3⁺CD8⁺ and CD3⁺CD4⁺ T cells were 36.8% and 56.9%, respectively (Table 1). According

Table 1. Frequencies of TIL Populations Expanded From GBM Tumors From Six Patients, Which Were Used in the Study

	CD3 ⁺	CD3 ⁺ / CD4 ⁺	CD3 ⁺ / CD8 ⁺	CD3 ⁺ / CD4 ⁺ CD8 ⁻	DP CD4 ⁺ CD8 ⁺
GBM-1	84.80	62.00	29.70	7.07	1.23
GBM-2	85.50	51.80	43.90	1.81	2.53
GBM-3	82.10	98.90	0.40	0.32	0.41
GBM-4	91.30	3.13	89.00	7.17	0.68
GBM-5	97.60	89.10	8.71	0.48	1.75
GBM-6	95.50	31.30	65.00	0.80	2.96
Median	88.40	56.90	36.80	1.31	1.49

TILs were expanded from glioma lesions and tested after a 4-week expansion phase with IL-2, IL-15, and IL-21. The majority of TILs are CD3⁺; the numbers for CD8⁺, CD4⁺, CD4⁺CD8⁻, and CD4⁺CD8⁺ represent the frequencies of the respective T-cell population among parental CD3⁺ T cells.

to the gating strategy established by Becattini et al.²⁸, TILs expanded from tumor tissue were highly Th1 polarized in the CD3⁺CD4⁺ subgroup; the median frequencies of Th1 (CCR6⁻CXCR3⁺CCR4⁻) and Th1* (CCR6⁺CXCR3⁺CCR4⁻) were 78.70% and 73.85%, respectively, along with intensely low Th2 and Th17 (median frequency lower than 1%). Th1* refers to non-conventional Th1, which shares great similarity to Th1, but besides interferon- γ (IFN- γ), Th1* cells also produce low levels of IL-17²⁷. TILs in the CD3⁺CD8⁻ and CD3⁺CD4⁺CD8⁻ subgroups express high levels of CXCR3 (median of 87.40% and 85.05%, respectively), a T-cell trafficking marker implicated in driving and establishing Th1 inflammation in sites of infection or tumor (Fig. 1). We observed a high expression of central memory T-cell immunophenotype markers (CD45RA⁻CCR7⁺) among CD3⁺CD4⁺, CD3⁺CD8⁺, and CD3⁺CD4⁺CD8⁻ T cells, with medians ranging from 34.75% to 42.9% (Fig. 2), potentially indicating longer survival and better prognosis in cancer. We then passed the cells through the intended microcatheter system with no effect on viability.

The animal experiments consisted of one positive control, two negative controls, four animals that received cell injections, and an additional two animals that received cell injections where the cells were marked for SPECT/CT tracking (Table 2). We started the animal experiments of the study with a positive control for ischemic embolization by bead injection ($n=1$). Control angiography following bead injection showed discontinued contrast passage in the middle cerebral artery (MCA). The beads caused significant cortical and subcortical lesions detected with DWI and corresponding apparent diffusion coefficient (ADC) maps. As an internal control, the contralateral hemisphere was used for evaluating MRI pulse sequences suitable for the rabbit brain, which were then used in the subsequent experiments.

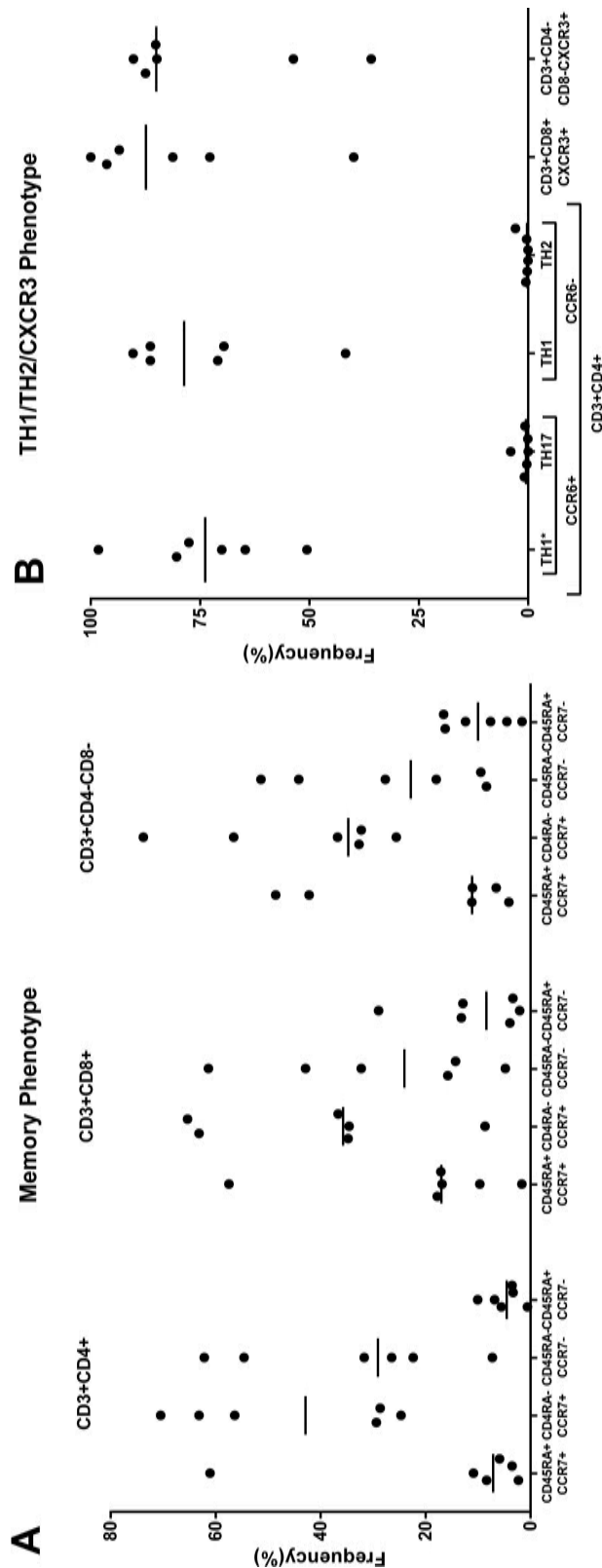


Figure 1. Cell phenotypes. (A) Frequency of T helper subpopulations (Th1*/Th1/Th2/Th17) among the CD4⁺ tumor-infiltrating lymphocyte (TIL) subpopulation and C-X-C chemokine receptor type 3 (CXCR3) expression in the CD8⁺ or CD4⁻CD8⁻ TIL subpopulation from the parental CD3⁺ T-cell group. CD4⁺ TILs are Th1 polarized (CXCR3⁺CCR4⁻), and the majority of CD8⁺ or CD4⁻CD8⁻ TILs reside in the CXCR3 T-cell subsets. (B) Frequency of T-cell populations (CD45RA and CCR7) in parental CD3⁺ TILs. The majority of TILs reside in the CD45RA⁻CCR7⁺ (effector memory) and CD45RA⁻CCR7⁻ (central memory) T-cell subsets. Each dot represents the TIL line from a single individual.

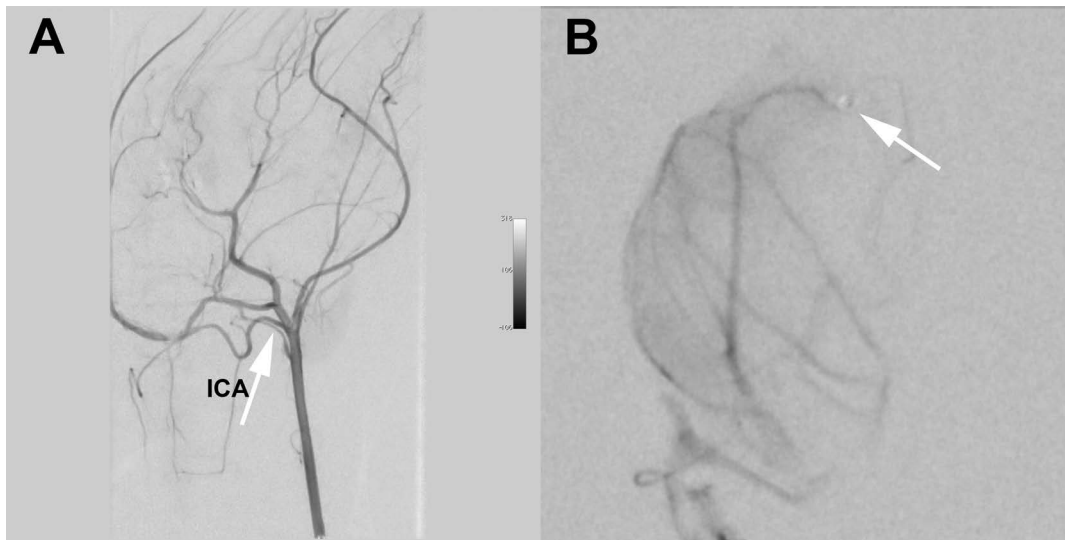


Figure 2. Angiography. (A) Lateral digital subtraction angiography (DSA) with the catheter tip in the common carotid artery (CCA) and the internal carotid artery (ICA) indicated by an arrow. (B) Posterior–anterior (PA) view DSA with a selective injection in the M1–M2 segment of the middle cerebral artery (MCA) after cell infusion, showing all major vessel branches with patent contrast flow. The arrow indicates the tip of the microcatheter. Note that the lenticulostriatal branches to the basal ganglia are too small in the rabbit to be detected with DSA.

In the next step, we performed diagnostic angiography with the microcatheter tip in the ICA segment ascending in the sphenoid fissure ($n=1$) and with the microcatheter tip in the M1 segment of the MCA as negative controls. No ischemic events were recorded. As previously described, the BBB opening was recorded with gadolinium-enhanced T1-weighted images.

The first cell-treated animal received cells with the microcatheter tip placed in the M1 segment (Fig. 2). Control angiography showed no large vessel occlusions compared to the positive control, and the MRI detected no infarction. In the second cell-treated animal, the microcatheter tip was advanced to the M2 segment to try to be even more selective with the injection. Again, no large vessel embolization or discontinuation of contrast passage could be identified. However, this animal suffered a small subcortical infarct in the lateral parts of the ipsilateral basal ganglia (Fig. 3), an area supported by small lateral lenticulostriatal branches originating

perpendicularly to the M1–M2 segment. Both animals showed gadolinium enhancement as an indication of BBB opening in a similar distribution as the negative control animal. The next two animals that were injected with cells were injected from the M1 segment without infarction. In total, three animals were injected with cells from the M1 segment without infarct, and one animal was injected with the microcatheter tip in the M2 segment. In the M2-injected animal, a small subcortical infarct in the basal ganglia was recorded.

To further evaluate the potential embolic–ischemic risks, two more animals were subject to injections in the ICA's horizontal segment of the carotid flexure, that is, with microcatheter placement more proximal to avoid direct mechanical obstruction of the perforating arteries by the catheter. In essence, we performed a selective injection to the frontal circulation of one hemisphere or a corresponding CNS volume of 3.5 cm^3 (Fig. 3). These cells were labeled with In^{111} , and following injection the

Table 2. Animal Distribution and MRI Results

No. of Animals	Procedure	MRI
1	Positive control with injection of beads	Infarcted in MCA territory
2	Control with only angiography, no cells	No infarcts
1	Cells in the M2 segment	Infarcted in basal ganglia (DWI verified)
3	Cells in the M1 segment	No infarct (DWI)
2	Cells in the ICA	No infarct (T2 at 24 h)

The number of animals per experimental procedure performed.

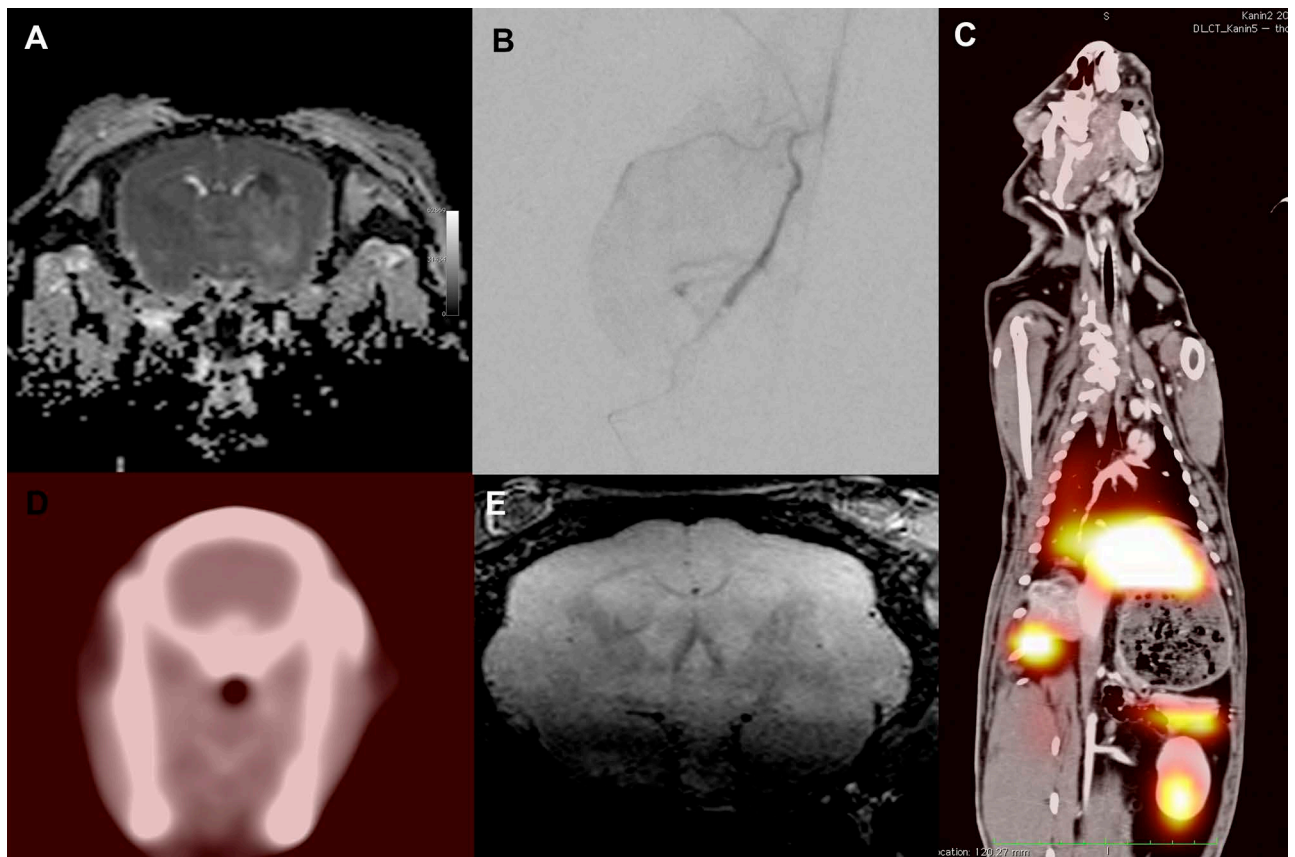


Figure 3. Magnetic resonance imaging (MRI) and single-photon emission computed tomography/computed tomography (SPECT/CT). (A) Coronal diffusion-weighted image (DWI) of the rabbit brain with a darker area in the lateral basal ganglia, indicating a recent ischemic insult from the second animal that was injected with the catheter tip in the M1–M2 segment. (B) Digital subtraction angiography (DSA) in posterior–anterior (PA) view with the microcatheter tip located in the internal carotid artery (ICA) with contrast detected in the middle cerebral artery (MCA), an azygos configured anterior cerebral artery (ACA), and the opticus artery (OA). (C) Negative SPECT/CT fusion axial section through the brain after selective injection of indium-111-labeled activated T cells. (D) Volumetric T2-weighted axial section at 24 h after cell injection without any indication of ischemic events. (E) SPECT/CT coronal fusion image with SPECT signal in the liver, spleen, pancreas, and kidney. Note that the mismatch between the SPECT and CT volumes is due to the SPECT images being collected over 60 min, and the CT images are obtained with a maximum inspiration.

animals were subject to SPECT/CT scanning. No SPECT signal above noise level was detected in the brains (Fig. 3). Thus, the epithelium of the healthy brain does not attract the activated T cells, and no mechanical embolization did occur. The majority of the SPECT signal was detected in the liver, the spleen, and, to some extent, the kidneys. No signal was detected in the lungs. Further, there was a small but clear uptake in the neck musculature of both animals.

On the subsequent day, we performed MRI scanning with a high-resolution (voxel size $0.20 \times 0.26 \times 0.26$ mm) 3D T2-weighted sequence (Fig. 3). No ischemic events were detected in any of the rabbits, while gadolinium enhancement could not be detected at 24 h.

DISCUSSION

When translating cell-based treatments in the clinical setting, a thorough preclinical evaluation is mandated.

In analogy to the proposed stem cell therapy as an emerging paradigm for stroke (STEPS) recommendation^{12,26}, a clearly defined cell population should be produced under GMP conditions, and cell populations should be tested in preclinical settings mimicking the proposed clinical trial. Further, when the proposed delivery mechanism is IA injection, an evaluation of the cells vis-à-vis the intended catheter system is also mandated. In this proof-of-concept study, we found IA delivery of TILs to be reasonably safe and feasible using healthy rabbits as an animal model.

Local delivery of TILs to the tumor lesions has been reported to be generally more clinically productive, whereby increased apoptosis of cancer cells and induction of CD4 and CD8 T cells are pronounced. Pertaining to intravenously delivered antigen-specific TILs that are retained in the lung, increased proportions of regulatory T cells can subdue tumor-specific T-cell activity locally,

thus allowing for tumor immune escape²⁹. Antigen-experienced TILs from lung metastases have also been shown to contain high numbers of effector memory (terminally differentiated) and lower numbers of central memory CD8 T cells³⁰. In addition, the 3-day lung retention of infused TILs may also lead to expansion of certain T-cell populations that may not be targeting the TAAs—as previously reported for a patient with metastatic colon cancer harboring a receptor tyrosine-protein kinase *erbB-2* (*ERBB2*) mutation³¹.

TILs expanded from GBM tumor tissue were highly Th1 polarized, concomitant with high surface expression of CXCR3 among the CD3⁺CD8⁺ or CD3⁺CD4⁻CD8⁻ subgroup. Based on previous findings^{32,33}, we are inclined to predict that the TILs would home to the tumor site, destroy the tumor-promoting microenvironment, and enable the “Th2-to-Th1” switch, which may induce tumor regression in patients. Furthermore, a high proportion of central memory T cells (CD45RA⁻CCR7⁺) in TILs (especially the CD3⁺CD8⁺ subgroup) may provide long-term antitumor activity, as they have been associated with better prognosis and longer patient survival^{34,35}. Thus, TILs expanded from tumor tissue *in vitro* may lead to durable antitumor effects due to their central memory phenotype, Th1 polarization, high CXCR3 expression, and tumor antigen specificity, while these benefits could be partly or entirely impaired due to the lung passage of the cells.

We chose to perform these safety studies in rabbit since it is possible to navigate to the CNS circulation with the smallest possible routinely available microcatheters. The CNS circulation of swine is inaccessible because of their *rete mirabili* under the skull base³⁶, and for ethical reasons, nonhuman primates were not deemed to be indicated.

The choice of rabbit as a model system most probably caused the ischemic lesion in the rabbit with the microcatheter tip in the M2 segment. The diameter of the tip and the geometry of the M1–M2 segment pointing laterally place the tip of the microcatheter against the superior vessel wall. This is the origination point of the phylogenetically highly conserved end-artery system to the basal ganglia. Thus, the tip of the catheter becomes wedged and mechanically obstructs the blood flow, leading to downstream ischemic events. In the other animals, where the catheter tip was placed more proximally in somewhat larger arterial dimensions, no infarction was detected by high-field diffusion-weighted MRI, accentuating the safety of the procedure and the cells in this clinically relevant experimental setup.

With the SPECT/CT, no cells could be detected in the brains of the animals. This has two implications. First, it appears highly unlikely that nonexistent cells caused the basal ganglia ischemic event in one animal and further strengthens catheter-induced mechanical obstruction of perforating arteries to the basal ganglia as an explanation.

Second, for normal brain, no apparent queues or signals appear to attract the activated T cells to induce homing of the cells.

An interesting and important finding in this study is that no SPECT signal could be detected in the lungs of the animals. This differs significantly from previous experiments with mesenchymal stromal cells, multipotent adult progenitor cells, bone marrow-derived mononuclear cells (BM-MNCs), and neural stem cells (NSCs)^{16,17,37}. Though not the primary subject of this study, it clearly warrants further research on the differences between, for instance, surface receptors between this population of activated T cells and other cell types.

The small but clearly detectable SPECT signal in the neck musculature of the animals could be either from a shunting steal from ICA branches or from the big venous drainage systems extracranially.

The inclusion of only six animals receiving cell injections in this study could be considered a shortcoming. However, these experiments are quite cumbersome, and the aims of the study were to evaluate the safety of IA TIL delivery and investigate whether this treatment may lead to catastrophic ischemic events. In relation to the abysmally poor prognosis of GBM patients, the authors consider this a sufficient number of large animals with full clinical integration to initiate clinical trials. The aim will then be to infuse tumor-activated T cells intra-arterially upstream to the GBM. It is widely accepted that the BBB is disrupted in GBM, and hopefully superselective injection of these aggressive cells could aggregate in the tumor area without causing severe systemic effects. The total cell dose could be reduced while achieving a high local cell concentration around the tumor.

Taken together, we have shown in the present study that 20 million activated T cells at a concentration of 4,000 cells/ μ l can be selectively infused to a CNS volume of 3.5 cm³ (estimated from the volumetric MRI) without catastrophic ischemic damage. The T cells passed through the brain without leaving SPECT signals and are initially retained in the liver largely followed by the spleen, pancreas, and kidneys. Virtually no uptake could be detected in the lungs. This indicates a big difference in biodistribution as opposed to other cell types, thus highlighting the potential of IA TIL delivery as a viable platform for cellular therapy.

ACKNOWLEDGMENTS: This study was supported by grants from the Karolinska Institutet funds, the Swedish Society of Medicine, The Swedish Brain Fund, HMT funding, Vinnova, Strokefonden, ALF funding (SLL), Uppdrag Besegra Stroke (Heart- and Lung Foundation and Karolinska Institutet), and the clinical post doc program from SLL. The funders had no role in the study design, data collection and analysis, decision to publish, or preparation of the manuscript. The authors thank Pellina Jansson and Johanna Doshé for excellent technical assistance. The authors declare no conflicts of interest.

REFERENCES

1. Stupp R, Hegi ME, Mason WP, van den Bent MJ, Taphoorn MJ, Janzer RC, Ludwin SK, Allgeier A, Fisher B, Belanger K, Hau P, Brandes AA, Gijtenbeek J, Marosi C, Vecht CJ, Mokhtari K, Wesseling P, Villa S, Eisenhauer E, Gorlia T, Weller M, Lacombe D, et al. Effects of radiotherapy with concomitant and adjuvant temozolomide versus radiotherapy alone on survival in glioblastoma in a randomised phase III study: 5-Year analysis of the EORTC-NCIC trial. *Lancet Oncol.* 2009;10(5):459–66.
2. Miao H, Choi BD, Suryadevara CM, Sanchez-Perez L, Yang S, De Leon G, Sayour EJ, McLendon R, Herndon JE, Healy P, Archer GE, Bigner DD, Johnson LA, Sampson JH. EGFRvIII-specific chimeric antigen receptor T cells migrate to and kill tumor deposits infiltrating the brain parenchyma in an invasive xenograft model of glioblastoma. *PLoS One* 2014;9(4):e94281.
3. Quattrocchi KB, Miller CH, Cush S, Bernard SA, Dull ST, Smith M, Gudeman S, Varia MA. Pilot study of local autologous tumor infiltrating lymphocytes for the treatment of recurrent malignant gliomas. *J Neurooncol.* 1999; 45(2):141–57.
4. Plautz GE, Miller DW, Barnett GH, Stevens GH, Maffett S, Kim J, Cohen PA, Shu S. T cell adoptive immunotherapy of newly diagnosed gliomas. *Clin Cancer Res.* 2000;6(6): 2209–18.
5. Plautz GE, Barnett GH, Miller DW, Cohen BH, Prayson RA, Krauss JC, Luciano M, Kangisser DB, Shu S. Systemic T cell adoptive immunotherapy of malignant gliomas. *J Neurosurg.* 1998;89(1):42–51.
6. Tsuboi K, Saijo K, Ishikawa E, Tsurushima H, Takano S, Morishita Y, Ohno T. Effects of local injection of ex vivo expanded autologous tumor-specific T lymphocytes in cases with recurrent malignant gliomas. *Clin Cancer Res.* 2003;9(9):3294–302.
7. Kitahara T, Watanabe O, Yamaura A, Makino H, Watanabe T, Suzuki G, Okumura K. Establishment of interleukin 2 dependent cytotoxic T lymphocyte cell line specific for autologous brain tumor and its intracranial administration for therapy of the tumor. *J Neurooncol.* 1987;4(4):329–36.
8. Tran E, Ahmadzadeh M, Lu YC, Gros A, Turcotte S, Robbins PF, Gartner JJ, Zheng Z, Li YF, Ray S, Wunderlich JR, Somerville RP, Rosenberg SA. Immunogenicity of somatic mutations in human gastrointestinal cancers. *Science* 2015;350(6266):1387–90.
9. Gubin MM, Zhang X, Schuster H, Caron E, Ward JP, Noguchi T, Ivanova Y, Hundal J, Arthur CD, Krebber WJ, Mulder GE, Toebes M, Vesely MD, Lam SS, Korman AJ, Allison JP, Freeman GJ, Sharpe AH, Pearce EL, Schumacher TN, Abersold R, Rammensee HG, et al. Checkpoint blockade cancer immunotherapy targets tumour-specific mutant antigens. *Nature* 2014;515(7528):577–81.
10. Meng Q, Liu Z, Rangelova E, Poiret T, Ambati A, Rane L, Xie S, Verbeke C, Doodoo E, Del Chiaro M, Lohr M, Segersvärd R, Maeurer MJ. Expansion of tumor-reactive T cells from patients with pancreatic cancer. *J Immunother.* 2016;39(2):81–9.
11. Bliss T, Guzman R, Daadi M, Steinberg GK. Cell transplantation therapy for stroke. *Stroke* 2007;38(2):817–26.
12. Wechsler L, Steindler D, Borlongan C, Chopp M, Savitz S, Deans R, Caplan L, Hess D, Mays RW, Boltze J, Boncoraglio G, Borlongan CV, Caplan LR, Carmicheal ST, Chopp M, Davidoff AW, Deans RJ, Fisher M, Hess DC, Kondziolka D, Mays RW, Norrving B, et al. Stem Cell Therapies as an Emerging Paradigm in Stroke (STEPS): Bridging basic and clinical science for cellular and neurogenic factor therapy in treating stroke. *Stroke* 2009;40(2):510–5.
13. Buckner CD, Clift RA, Fefer A, Lerner KG, Neiman PE, Storb R, Thomas ED. Marrow transplantation for the treatment of acute leukemia using HL-A-identical siblings. *Transplant Proc.* 1974;6(4):365–6.
14. Thomas E, Storb R, Clift RA, Fefer A, Johnson FL, Neiman PE, Lerner KG, Glucksberg H, Buckner CD. Bone-marrow transplantation (first of two parts). *New Engl J Med.* 1975;292(16):832–43.
15. Thomas ED, Storb R, Clift RA, Fefer A, Johnson L, Neiman PE, Lerner KG, Glucksberg H, Buckner CD. Bone-marrow transplantation (second of two parts). *New Engl J Med.* 1975;292(17):895–902.
16. Fischer UM, Harting MT, Jimenez F, Monzon-Posadas WO, Xue H, Savitz SI, Laine GA, Cox CS Jr. Pulmonary passage is a major obstacle for intravenous stem cell delivery: The pulmonary first-pass effect. *Stem Cells Dev.* 2009;18(5):683–92.
17. Lappalainen RS, Narkilahti S, Huhtala T, Liimatainen T, Suuronen T, Närvänen A, Suuronen R, Hovatta O, Jolkkonen J. The SPECT imaging shows the accumulation of neural progenitor cells into internal organs after systemic administration in middle cerebral artery occlusion rats. *Neurosci Lett.* 2008;440(3):246–50.
18. Fisher B, Packard BS, Read EJ, Carrasquillo JA, Carter CS, Topalian SL, Yang JC, Yolles P, Larson SM, Rosenberg SA. Tumor localization of adoptively transferred indium-111 labeled tumor infiltrating lymphocytes in patients with metastatic melanoma. *J Clin Oncol.* 1989;7(2):250–61.
19. Tseng J, Citrin DE, Waldman M, White DE, Rosenberg SA, Yang JC. Thrombotic microangiopathy in metastatic melanoma patients treated with adoptive cell therapy and total body irradiation. *Cancer* 2014;120(9):1426–32.
20. Qian C, Yan H, Hu X, Zhang W, Liu H. Increased risk of venous thromboembolism in patients with brain tumors: A systematic review and meta-analysis. *Thromb Res.* 2016; 137:58–63.
21. Ben-Haim S, Asaad WF, Gale JT, Eskandar EN. Risk factors for hemorrhage during microelectrode-guided deep brain stimulation and the introduction of an improved microelectrode design. *Neurosurgery* 2009;64(4):754–63.
22. Lundberg J, Le Blanc K, Söderman M, Andersson T, Holmin S. Endovascular transplantation of stem cells to the injured rat CNS. *Neuroradiology* 2009;51(10):661–7.
23. Jin K, Sun Y, Xie L, Mao XO, Childs J, Peel A, Logvinova A, Banwait S, Greenberg DA. Comparison of ischemia-directed migration of neural precursor cells after intrastriatal, intraventricular, or intravenous transplantation in the rat. *Neurobiol Dis.* 2005;18(2):366–74.
24. Willinsky RA, Taylor SM, TerBrugge K, Farb RI, Tomlinson G, Montanera W. Neurologic complications of cerebral angiography: Prospective analysis of 2,899 procedures and review of the literature. *Radiology* 2003;227(2):522–8.
25. Takayama T, Makuuchi M, Sekine T, Terui S, Shiraiwa H, Kosuge T, Yamazaki S, Hasegawa H, Suzuki K, Yamagata M, and others. Distribution and therapeutic effect of intraarterially transferred tumor-infiltrating lymphocytes in hepatic malignancies. A preliminary report. *Cancer* 1991;68(11):2391–6.
26. Renú A, Amaro S, Laredo C, Román LS, Llull L, Lopez A, Urra X, Blasco J, Oleaga L, Chamorro Á. Relevance of blood-brain barrier disruption after endovascular treatment

- of ischemic stroke: Dual-energy computed tomographic study. *Stroke* 2015;46(3):673–9.
27. Savitz SI, Chopp M, Deans R, Carmichael T, Phinney D, Wechsler L, STEPS Participants. Stem cell therapy as an emerging paradigm for stroke (STEPS) II. *Stroke* 2011;42(3):825–9.
 28. Becattini S, Latorre D, Mele F, Foglierini M, De Gregorio C, Cassotta A, Fernandez B, Kelderman S, Schumacher TN, Corti D, Lanzavecchia A, Sallusto F. T cell immunity. Functional heterogeneity of human memory CD4⁺ T cell clones primed by pathogens or vaccines. *Science* 2015;347(6220):400–6.
 29. Kurose K, Ohue Y, Sato E, Yamauchi A, Eikawa S, Isobe M, Nishio Y, Uenaka A, Oka M, Nakayama E. Increase in activated Treg in TIL in lung cancer and in vitro depletion of Treg by ADCC using an antihuman CCR4 mAb (KM2760). *J Thorac Oncol*. 2015;10(1):74–83.
 30. Turcotte S, Gros A, Hogan K, Tran E, Hinrichs CS, Wunderlich JR, Dudley ME, Rosenberg SA. Phenotype and function of T cells infiltrating visceral metastases from gastrointestinal cancers and melanoma: Implications for adoptive cell transfer therapy. *J Immunol*. 2013;191(5):2217–25.
 31. Morgan RA, Yang JC, Kitano M, Dudley ME, Laurencot CM, Rosenberg SA. Case report of a serious adverse event following the administration of T cells transduced with a chimeric antigen receptor recognizing ERBB2. *Mol Ther*. 2010;18(4):843–51.
 32. Groom JR, Luster AD. CXCR3 in T cell function. *Exp Cell Res*. 2011;317(5):620–31.
 33. Hickman HD, Reynoso GV, Ngudiankama BF, Cush SS, Gibbs J, Bennink JR, Yewdell JW. CXCR3 chemokine receptor enables local CD8(+) T cell migration for the destruction of virus-infected cells. *Immunity* 2015;42(3):524–37.
 34. Klebanoff CA, Gattinoni L, Restifo NP. CD8+ T-cell memory in tumor immunology and immunotherapy. *Immunol Rev*. 2006;211(1):214–24.
 35. Klebanoff CA, Gattinoni L, Torabi-Parizi P, Kerstann K, Cardones AR, Finkelstein SE, Palmer DC, Antony PA, Hwang ST, Rosenberg SA, Waldmann TA, Restifo NP. Central memory self/tumor-reactive CD8+ T cells confer superior antitumor immunity compared with effector memory T cells. *Proc Natl Acad Sci USA* 2005;102(27):9571–6.
 36. Gralla J, Schroth G, Remonda L, Fleischmann A, Fandino J, Slotboom J, Brekenfeld C. A dedicated animal model for mechanical thrombectomy in acute stroke. *Am J Neuro-radiol*. 2006;27(6):1357–61.
 37. Arnberg F, Lundberg J, Kenne E, Jaff N, Müller P, Nava S, Kaibe H, Ringden O, Holmin S. Superselective intra-arterial umbilical cord blood administration to BM in experimental animals. *Bone Marrow Transpl*. 2014;49(12):1486–91.